Published in: Chemical Physics (1987), vol. 117, pp. 305-313.
Status: Postprint (Author's version)

A MASS SPECTROMETRIC PHOTOIONIZATION STUDY OF CH_3F. THE CH_2^+, CH_3^+ AND CH_2F^+ ION FORMATION

R. LOCHT, J. MOMIGNY

Département de Chimie Générale et de Chimie Physique, Institut de Chimie, Bâtiment B6, Université de Liège, Sart-Tilman B-4000 Liège 1, Belgium

E. RÜHL and H. BAUMGARTEL

Institut für Physikalische und Theoretische Chemie, Freie Universität Berlin, Takustrasse 3, D-1000 Berlin 33, Germany

Abstract

The decay of CH_3F^+ in the CH_2^+, CH_3^+ and CH_2F^+ dissociation channels has been investigated by photoionization mass spectrometry using synchrotron radiation in the energy range 10-25 eV. The photoabsorption curve of CH_3F and the ionization efficiency curves of CH_2^+, CH_3^+ and CH_2F^+ as well as the translational energy spectra and the kinetic energy versus appearance energy diagram for CH_3^+ were recorded. For the three fragment ions dissociative autoionization is a prominent formation process. Direct dissociative ionization is observed for the same ions through the decomposition of the CH_3F^+ ($\tilde{A}^2A_1$ + $\tilde{B}^2E$) state at 16.1 eV as well as presumably of the $\tilde{C}^2A_1$ state at about 22.5 eV.

1. Introduction

Early dissociative electroionization [1] and mass spectrometric photoionization [2] studies were concerned with the CH_3^+ ion formation from CH_3F. Both experiments gave evidence for ion-pair formation at 12.59 eV and dissociative ionization at 16.25 eV [2]. The former showed an additional process with an onset at 14.7 eV [1] while no ion current was detected at this energy in the latter.

In a kinetic energy distribution study of the CH_3^+ ion [1], "thermal" and "nearly thermal" ions were correlated with the 12.59 and 14.5 eV thresholds [1] and the "energetic" CH_3^+ ions were found to have their onset at 16.2 eV [1]. A photo-electron-photoion coincidence work confirmed the formation of the energetic CH_3^+ ions at 16.5 eV only [3].

The CH_3^+ ion production from CH_3F has recently been reinvestigated by dissociative electroionization with ion energy analysis [4]. Under non-coincidence conditions, a fixed wavelength photoionization experiment [4,5] using the HeI (58.4 nm) and NeI (73.58-74.37 nm) resonance lines showed "thermal" as well as "energetic" CH_3^+ ions at both wavelengths, in agreement with the electroionization results. The two components of the ion kinetic energy distribution have about the same integrated intensity.

In this paper the dissociative photoionization of CH_3F has been investigated by using synchrotron radiation. The aim of this work is to elucidate the discrepancies between electroionization and photoionization as far as the CH_3^+ ion formation is concerned. The CH_2^+ ion is detected with a reasonable intensity in the photoionization mass spectrum. Therefore its ionization efficiency has been recorded and will be compared to the corresponding electroionization results [4]. Furthermore the ionization efficiency curves of CH_3F^+ and CH_2F^+ as well as the photoabsorption curve of CH_3F were recorded to enlighten the interpretation and discussion of the results on CH_2^+ and CH_3^+.

Simultaneously this experiment provided the opportunity to apply to photoionization the same technique as the one used in electroionization [4]. It consists of building a kinetic-energy versus appearance-energy diagram by recording the ionization efficiency curves of energy-selected fragment ions. The investigation of the dissociative ionization of CH_3F is chosen to test the method.

Published in: Chemical Physics (1987), vol. 117, pp. 305-313.
Status: Postprint (Author's version)

2. Experimental

The experimental setup used in the present work is nearly the same as the one used in the electroionization and fixed-wavelength photoionization experiments described elsewhere [5,6]. The main differing feature in the present work is the use of the synchrotron radiation of the Berlin electron storage ring BESSY as a light source. This radiation is dispersed by a 1 m normal incidence monochromator (McPherson 225) with a wavelength resolution set at 0.4 nm.

After photoionization the ions are extracted by a weak drawout field, focused on the exit hole of the ion source, energy analysed by a retarding lens and accelerated into a quadrupole filter for mass analysis. The ion current, collected in a chan-neltron multiplier, is continuously scanned as a function of either the photon wavelength at fixed retarding potential V_R or the retarding potential at fixed photon energy hv. The first derivative of the retarding potential curves is obtained numerically.

The photoabsorption curve has been recorded using a windowless, single beam absorption cell and the light is detected by a photomultiplier. The spectra are recorded at a typical 0.1 nm resolution.

The methyl fluoride gas, purchased from PCR (USA) was used without further purification. The sample is introduced at a pressure of about 10^{-5} Torr.

The photon count rate is monitored by a sodium salicylate sensitized photomultiplier. This reference count rate is used for the normalization of photoionization efficiency curves.

The maximum of the CH_3F^+ ion translational energy distribution is used as the zero-energy calibration point for the ion translational energy scale. The same reference is used during the recording of the photoionization efficiency curve of CH_3^+ at different retarding potential settings.

3. Results

The photoabsorption curve of CH_3F has been recorded from 7 to 30 eV. Only the energy range of interest, i.e. 10-25 eV is reproduced in figs. 1a and 2a. An extensive vibrational structure is observed at the low-energy side of this spectrum, i.e. 10-13 eV, and the photoabsorption curve is dominated by several broad and structureless bands at higher energies.

Harshbarger et al. [7] published an extensive study of the electron energy-loss spectra of fluo-roalkanes. The interpretation of their spectra is made in terms of Rydberg transitions, based on term value assignments. Table 1 displays the vertical energies of the features observed in figs. 1a and 2a and the corresponding assignment of Harshbarger et al. [7].

The photoionization efficiency curves of CH_3F^+ and CH_2F^+ are shown in figs, 1b and lc respectively. Comparing these results with the early photoionization work of Krauss et al. [2], we see that several features are more clearly shown in evidence in the present work. For the CH_3F^+ parent ions, appearing at 12.50 ± 0.03 eV, broad and very likely structureless peaks are observed in the energy ranges 13.6-15.4 eV, 15.3-19 eV and 19-22 eV. For comparison, the Franck-Condon regions for the three electronic states of CH_3F^+, as observed by He(I) and He(II) photoelectron spectroscopy [8,9], are inserted in fig. lb.

For the CH_2F^+ ion, the photoionization efficiency curve with the lowest onset at 13.35 ± 0.03 eV, shows better defined peaks with their maxima at 14.13 ± 0.04 eV, 15.40 ± 0.06 eV (with a shoulder at 15.13 eV) and 20.5 ± 0.1 eV. A slow but noticeable increase of the ionization efficiency is observed at 17.20 ± 0.06 eV. The first two features are present in the results published by Krauss et al. [2].

The photoionization efficiency curve of the CH_2^+ ion, displayed in fig. 2c, has been recorded for comparison with the electron-impact work on the same ion [4]. Owing to its low intensity, the photoionization efficiency of CH_2^+ as a function of the photon energy has only been measured at a slightly negative retarding potential setting. Well defined onsets are measured at 13.90 ± 0.06 eV, 14.63 ± 0.04 eV and at 22.36 ± 0.06 eV. Increases of the ionization efficiency are also observed at about 17.2 and 21 eV.

For clarity in the following discussion, the ionization efficiency curve of CH_3^+, as recorded at a slightly negative retarding potential, as well as the photoabsorption curve of CH_3F, are displayed in figs. 2b and 2a respectively.

Published in: Chemical Physics (1987), vol. 117, pp. 305-313.
Status: Postprint (Author's version)

The translational energy distributions of CH_3^+, as given by the first derivative of the retarding potential curves, were recorded at different wavelengths between 72 and 49 nm (16.4-25 eV). Fig. 3 shows a number of kinetic energy distributions for photon energy settings located by arrows in fig. lb, where the photoionization efficiency curve of CH_3F^+ is reproduced.

In the photon energy range 17.3-21.22 eV, the CH_3^+ translational energy distributions show two components: (i) a "thermal" CH_3^+ ion energy distribution and (ii) an "energetic" CH_3^+ ion energy component peaking at 0.8 eV. When it extends up to about 1.5 eV for 17.3 eV (71.7 nm) photon energy, the CH_3^+ translational energy distribution is remarkably constant between 18.9 and 21.2 eV (65.2-58.4 nm) photon energy, spreading up to 1.8 eV. At 16.4 eV (75.6 nm) mainly the thermal energy distribution of the CH_3^+ ion is observed. These observations are in good agreement with the electron-impact [4] and fixed-wavelength photoionization results [4,5].

Fig. 1. *The photoabsorption curve of CH_3F (a) and the photoionization efficiency curves of CH_3F^+/CH_3F (b) and CH_2F^+/CH_3F (c). The horizontal lines are related to the He(I) and He(II) photoelectron spectra of the $\tilde{X}^2E$, the $(\tilde{A}^2A_1 + \tilde{B}^2E)$ and the $\tilde{C}^2A_1$ states of CH_3F. The arrows locate the photon energies where the kinetic energy distribution of CH_3^+ is measured.*

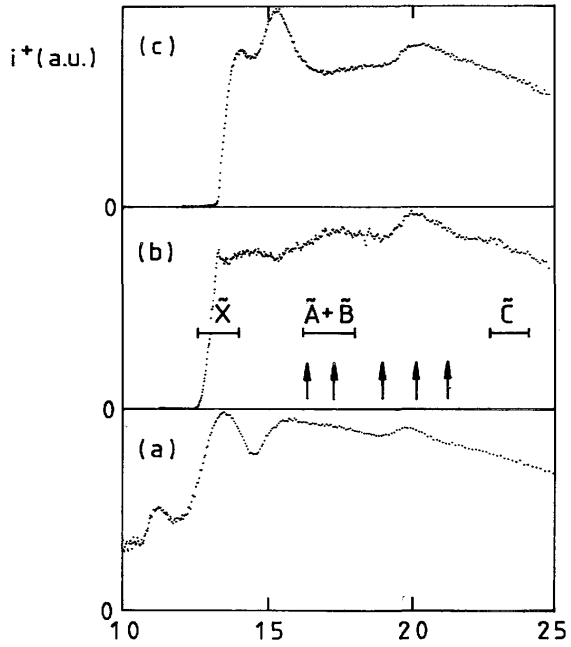

Table 1. *Vertical excitation energies (EE_{vert}), vertical ionization energies (IE_{vert}) [8] (eV) and assignments [7] for methyl fluoride: (s) refers to shoulders in the corresponding bands*

EE_{vert}	IE_{vert}	Assignment
11.20		2e → 4s or valence shell excitation
	13.03	$(2e)^{-1}$
13.5		le, $5a_1$ → 3s
13.7(s)		
15.25		le, $5a_1$ → 4s
15.55		σ(C-H) → σ*(C-H) valence shell excitation
	17.02	$(1e, 5a_1)^{-1}$
19.80		$4a_1$ → 3s
20.4 (s)		
22.3 (s)		
	23.4	$(4a_1)^{-1}$

Published in: Chemical Physics (1987), vol. 117, pp. 305-313.
Status: Postprint (Author's version)

Fig. 2. *The photoabsorption curve of CH_3F (a) and the photoionization efficiency curves of CH_3^+/CH_3F (b) and CH_2^+/CH_3F (c) as observed at a slightly negative retarding potential.*

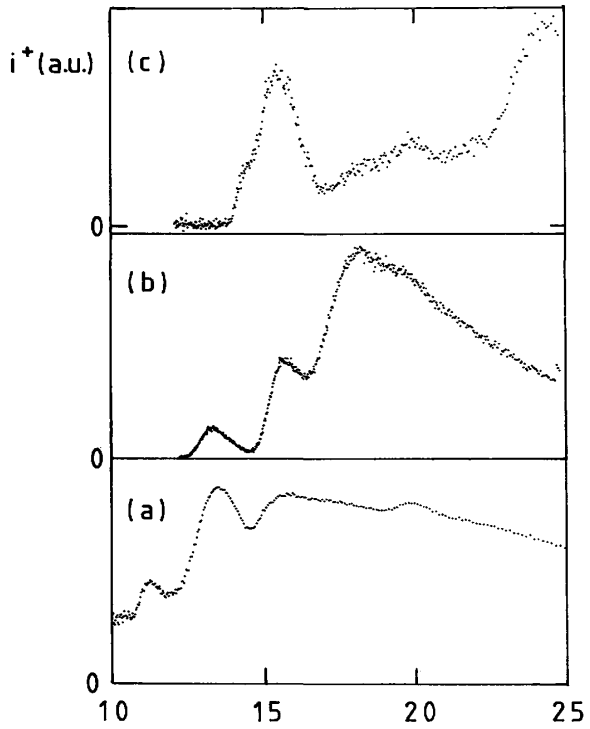

Fig. 2b and 4 show the photoionization efficiency curves of the CH_3^+ ion at different retarding potential settings. The ionization efficiency of CH_3^+ could not be recorded above V_R = 1.2 V because of large intensity losses. For V_R = — 0.4 V (see fig. 2b) clearly three onsets are observed, i.e. at 12.45 ± 0.06 eV, 14.50 ± 0.06 eV and around 16.4 eV. The process at 14.60 eV, not detected in an earlier photoionization work [2], is clearly visible in the present experiment. This process overlaps the third onset at 16.40 eV. This threshold shifts down to 16.10 ±0.06 eV for higher retarding potential settings where the lower-lying process is suppressed.

For the easiness of the following discussion, the most important features observed in the photoionization efficiency curves of the abovemen-tioned ions are listed in table 2.

Table 2. *Synoptic table of the most important features in the photoionization efficiency curves of CH_3F^+, CH_2F^+, CH_3^+ and CH_2^+ from CH_3F: (o) = onset, (bs) = broad structure, (m) = maximum*

CH_3F^+	12.50(o)	13.6-15.4(bs) 15.3-19(bs) 19-22(bs)	
CH_2F^+		13.5 (o)-14.13(m)-15.40(m) 20.5(m)	17.2(o)
CH_3^+	12.45(o)	14.50(o) 19-22(bs)	16.10(o)
CH_2^+		13.90(o)-14.63(o)-15.4(m) 22.36(o)	17.2(o)

4. Discussion

4.1. The CH_2F^+ dissociation channel

Photoelectron-photoion coincidence work [3] unambiguously showed these ions to appear at the energy of the second Jahn-Teller component of the $CH_3F^+(\tilde{X}^2E)$ state. Furthermore, the photo-ionization efficiency curve shows (see fig. 1c) significant contributions due to the autoionization of Rydberg (le, $5a_1 \rightarrow 3s$), (le, $5a_1 \rightarrow 4s$)

Published in: Chemical Physics (1987), vol. 117, pp. 305-313.
Status: Postprint (Author's version)

and ($4a_1 \rightarrow 3s$) states converging to the ionization limits of the (le, $5a_1$) and the ($4a_1$) orbitals of CH_3F. This is evidenced by the maximum at 14.13 eV which lies in the energy range covered by the 13.5 eV (le, $5a_1 \rightarrow 3s$) absorption band. Besides, broad peaks are observed at about 15.4 eV (le, $5a_1 \rightarrow 4s$) and 20.5 eV ($4a_1 \rightarrow 3s$). These features look essentially structureless.

Fig. 3. *The numerical first derivative of the retarding potential curves of CH_3^+/CH_3F as recorded at (a) 75.6 nm, (b) 71.7 nm, (c) 65.2 nm, (d) 61.4 nm, (e) 58.4 nm. The fine structure is spurious.*

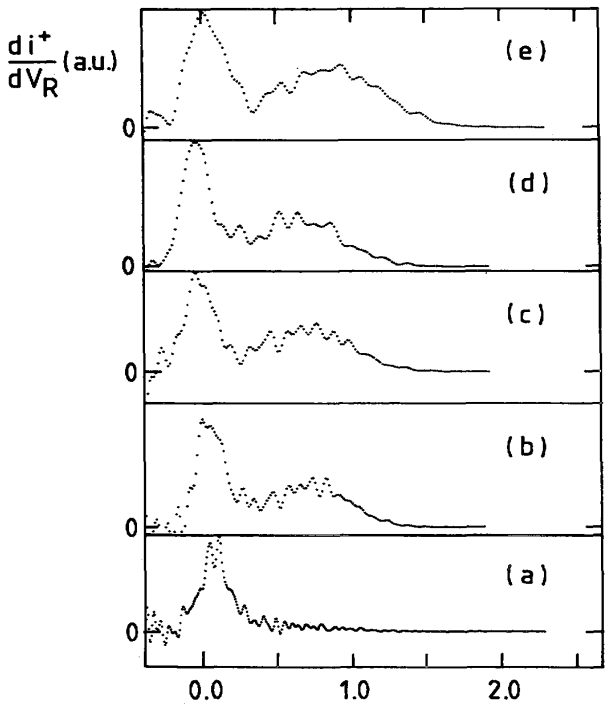

Fig. 4. *The photoionization efficiency curves of CH_3^+/CH_3F recorded at different retarding potential settings V_R: (a) — 0.40 V, (b) 0.19 V, (c) 0.45 V, (d) 0.70 V, (e) 0.96 V and (f) 1.2 V.*

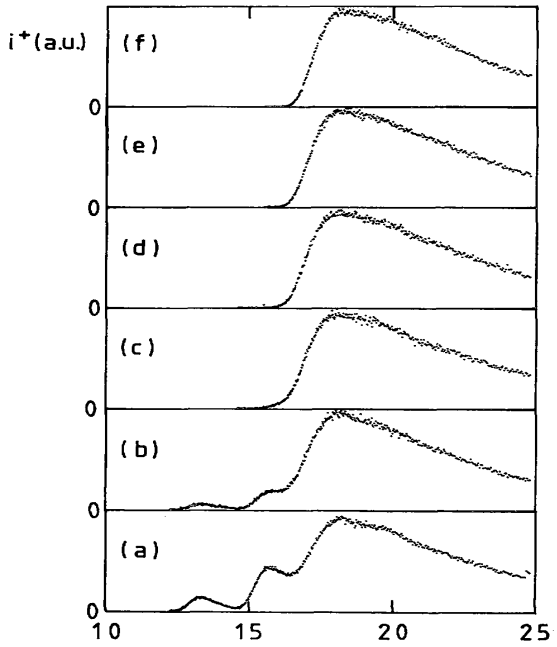

Published in: Chemical Physics (1987), vol. 117, pp. 305-313.
Status: Postprint (Author's version)

The second autoionization peak, with a maximum at 15.6 eV and a shoulder on the low-energy side (at about 15.2 eV), spreads over the energy range 14.5-17 eV. As will be seen in the following discussion, the Rydberg (le, $5a_1 \rightarrow 4s$) transition plays also an important role in the dissociative ionization of CH_3F in both the CH_3^+ and CH_2^+ channels. On the other hand, it has to be noticed that no structure corresponding to this state is found in the ionization efficiency curve of CH_3F^+ where a dip is observed at 15.5 eV (see fig. lb).

A slow but significant increase in the photo-ionization efficiency of CH_2F^+ is observed at 17.2 eV. The energy difference of 3.85 eV, between 17.2 eV and the lowest onset at 13.35 eV, can be compared with the energy separation of 3.49 eV between the lowest singlet states $\tilde{X}\,^1A_1$ and $\tilde{A}\,^1A''$ of H_2CO, isoelectronic species of CH_2F^+ [10].

The threshold at 17.2 eV lies in the energy range of the $CH_3F^+(\tilde{A}^2A_1 + \tilde{B}^2E)$ photoelectron band. As will be noticed below dissociation channels corresponding to the production of CH_2^+ and CH_3^+ are open at the same energy. However, by photoelectron-photoion coincidence spectroscopy [3], no coincidences are measured between CH_2F^+ ions and electrons corresponding to the $(\tilde{A}^2A_1 + \tilde{B}^2E)$ band. Consequently, the dissociation limit at 17.2 eV, leading to $CH_2F^+(\tilde{A}\,^1A'')$ ions, would be populated through autoionization.

4.2. The CH_2^+ dissociation channel

Though the overall shape of the photoioniza-tion efficiency curve (see fig. 2c) is comparable to the first differentiated electroionization efficiency curve [4], well resolved details are observed in the present work. Two closely lying onsets are observed by photoionization, i.e. 13.90 ± 0.06 eV and 14.63 ± 0.06 eV. These two processes being not resolved by electron impact, only an average onset of 14.3 ± 0.1 eV was measured [4].

The lowest threshold for the CH_2^+ ion production from CH_3F by the mechanism

$$\mathbf{CH_3F + h\nu \rightarrow CH_2^+(\tilde{X}\,^2A_1) + HF(X\,^1\Sigma^+) + e^-,} \quad (1)$$

is calculated at 13.9 ± 0.4 eV (based on thermodynamical and spectroscopic data given in table 1 of ref. [4]), in very good agreement with the experimental measurement. The CH_2^+ ion is known to be formed without translational energy at the onset by electron impact as well as by photoionization with the HeI and the NeI resonance lines [4].

The first onset for the appearance of the CH_2 ion lies in the $CH_3F^+(\tilde{X}\,^2E)$ state energy range extending from 12.533 to 14.5 eV. An extensive vibrational structure is observed in the corresponding photoelectron band [8]. A sudden breakdown in the intensity distribution, corresponding to the second Jahn-Teller component, is observed at about 13.32 eV, i.e. the onset energy measured for the appearance of CH_2F^+ [2,3]. The vibrational structure becomes diffuse at 13.8 eV corresponding fairly well to the appearance energy of CH_2^+.

The energy difference between the two first processes is 14.63 - 13.90 = 0.73 eV. The most obvious interpretation of the onset at 14.63 eV would be

$$\mathbf{CH_2F + h\nu \rightarrow CH_2^+(\tilde{A}^2B_1) + HF(X\,^1\Sigma^+) + e^-,} \quad (2)$$

where the CH_2^+ ion is formed in its first excited $\tilde{A}^2B_1$ state. Considering the isoelectronic BH_2 species, the first electronic excited state is at 0.6 eV above the ground state [10]. However, by quantum mechanical calculations on the CH_2^+ system [11], this energy is estimated to be about 0.13 eV. The CH_2^+ producing process does not involve translational energy of the fragments and has to occur through dissociative autoionization.

This interpretation is supported by two arguments. Firstly, the CH_2^+ photons are known to be thermal in the photon energy range covered by the Ne(I) resonance line [4]. On the other hand, between 14.5 eV, i.e. the upper end of the $\tilde{X}^2E$ photoelectron band, and about 16.3 eV, corresponding to the adiabatic ionization energy of the $\tilde{A}^2A_1 + \tilde{B}^2E$ state, no direct ionization cross section is measured for CH_3F. However, in the energy range 14.5-14.6 eV dissociative ionization channels are open, leading to CH_2F^+, CH_3^+ and CH_2^+ ions. A peak rising at 14.63 eV, has its maximum at 15.4 eV and extends to at least 17.0 eV. This feature corresponds to the same structure observed at the same energy, i.e. the (1e, $5a_1 \rightarrow 4s$) band in the photoabsorption curve of CH_3F (fig. 2a) and in the photoionization efficiency curve of CH_2F^+ (fig. 1c).

Published in: Chemical Physics (1987), vol. 117, pp. 305-313.
Status: Postprint (Author's version)

When a slight increase of the CH_2^+ photoion current is observed around 21 eV, the cross section significantly increases at 22.36 ± 0.06 eV. The same features were observed in the electroionization efficiency curve 21.4 ± 0.2 eV and at 23.4 ± 0.1 eV [4].

The present photoionization measurement, together with the kinetic-energy versus appearance-energy diagram of CH_2^+ [4], enable us to make a more precise energy balance. For 23.4 eV electrons the CH_2^+ ions carry more than 0.6 eV translational energy. For 25 eV electrons [4], the ion energy distribution spreads up to 1.7 eV, i.e. 1.7 X 34/20 = 2.9 eV total translational energy. Assuming that the total excess energy is entirely converted into translational energy of the fragments, the "zero kinetic energy onset" would be at 25.0 — 2.9 = 22.1 eV which has to be compared with the measured onset of 22.36 eV. The minimum energy required for the process

$$CH_3F + h\nu \rightarrow CH_2^+(\tilde{X}\,^2A_1) + H(^2S_g) + F(^2P_u) + e^- \quad (3)$$

is calculated at 19.8 ± 0.3 eV [4]. The energy difference, i.e. 22.1 - 19.8 = 2.3 eV, has to be ascribed to vibronic excitation of CH_2^+. Quantum mechanical calculations [12] showed a $\tilde{B}^2B_2$ and an $\tilde{a}\,^4A_2$ state of CH_2^+ at 3.6 and 3.5 eV respectively above the $\tilde{X}\,^2A_1$ ground state. Furthermore, the appearance energy of 22.36 eV corresponds fairly well to the adiabatic ionization energy of 22.5 eV determined for the $CH_3F^+(\tilde{C}\,^2A_1)$ state [9].

However, in the photoabsorption curve of CH_3F (see fig. 2a), besides a well defined peak with a maximum at 19.8 eV, shoulders have to be noticed at about 20.4 eV and a very weak band near 22.3 eV. The latter could be correlated with the appearance onset for CH_2^+. This would at least imply that the CH_2^+ ion is partly produced by dissociative autoionization at this energy.

The photoionization efficiency of CH_2^+ shows very smooth variations between 17 and 22 eV. However, "onsets" near 17.2 eV and 21 eV are observed. CH_2^+ being produced without kinetic energy in this energy range [4], this ion is probably formed via mechanism (1), but where CH_2^+ is excited in higher vibronic states. The $CH_2^+(\tilde{B}^2B_2)$ state has been calculated at 3.2 eV [13] or 3.6 eV [12] above the ground state. The corresponding onset would be at 17.1-17.5 eV and lies in the $CH_3F^+(\tilde{A}^2A_1 + \tilde{B}^2E)$ states' energy range. As mentioned earlier in this section, a slight increase in the ionization efficiency curve of CH_2F^+ is observed at the same energy. It was also noticed that no photoelectron-photoion coincidence was observed between this ion and $(\tilde{A}^2A_1 + \tilde{B}^2E)$ photoelectrons [3].

Besides the onset of 17.2 eV, fairly well defined peaks at about 20 and 21.5 eV are observed. The presence of the former feature has been mentioned in the ionization efficiency curves of CH_3F^+ and CH_2F^+ (see figs, 1b and 1c). This observation strongly suggests that these structures are related to dissociative autoionization at the expense of a member of a Rydberg series converging to the $\tilde{C}\,^2A_1$ state of CH_3F^+, e.g. ($4a_1 \rightarrow 3s$) transition. At about 21 eV enough energy is available to open the dissociation channel (3) without kinetic energy of the fragments, all species being in their ground state.

As for electroionization, no evidence is found in the photoionization efficiency curve of CH_2^+ for the ion-pair production

$$CH_3F + h\nu \rightarrow CH_2^+(\tilde{X}\,^2A_1) + H(^2S_g) + F^-(^1S_g), \quad (4)$$

which would have its threshold at 16.4 ± 0.3 eV [4]. Probably this process has a low cross section and could not be observed in the ionization efficiency curve shown in fig. 2c.

4.3. The CH_3^+ dissociation channel

The CH_3^+ photoionization efficiency curve yields onset measurements which are in close agreement with the electron impact results [4]. Fig. 5 displays the kinetic-energy versus appearance energy plot obtained in the present work. The dotted lines drawn in this figure represent the corresponding diagram obtained by electron impact. Owing to the better resolution obtained by photoionization, the threshold shift as a function of the retarding potential for the second process, i.e. with the onset at 14.50 ± 0.06 eV, is measured up to V_R = 0.7 V. By electroionization it was only observed up to 0.2 V.

Published in: Chemical Physics (1987), vol. 117, pp. 305-313.
Status: Postprint (Author's version)

Fig. 5. *The kinetic-energy versus appearance-energy diagram for CH_3^+/CH_3F. Dotted lines represent the electroionization results.*

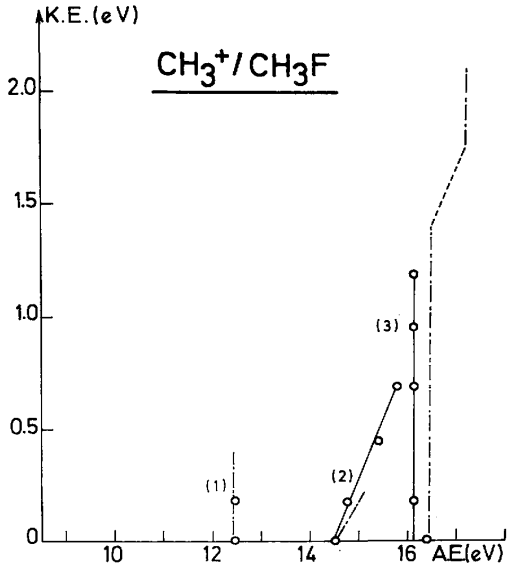

The first onset at 12.45 ± 0.06 eV has to be unambiguously ascribed to the ion-pair formation

$$CH_3F + h\nu \rightarrow CH_3^+\left(\tilde{X}\,^1A_1'\right) + F^-\left(^1S_g\right), \quad (5)$$

for which the thermodynamic threshold is calculated at 11.2 ± 0.3 eV [4]. The kinetic-energy versus appearance-energy diagram related to this process (vertical line (1) in fig. 5) has to be interpreted by the 1.25 eV excess energy partition between internal energy of CH_3^+ and translational energy of the fragments CH_3^+ and F^-. The CH_3^+ ion detection below 12.4 eV was unsuccessful as it was by electron impact [4]. Consequently the two thresholds reported by Tsuda et al. [14] at 10.8 and 11.9 eV could not be confirmed.

The ion-pair process is known to occur often through predissociation involving neutral states with Rydberg character. In the present case, the ion-pair onset lies in the energy range of the (le, $5a_1 \rightarrow 3s$) Rydberg state of CH_3F. This state spreads from 12-14.5 eV and peaks at 13.45 eV. The low-energy side of this peak exhibits a complex vibrational structure with a 120 meV spacing, corresponding fairly well to the ν_6 vibrational mode of the $CH_3F^+(\tilde{X}\,^2E)$ state [8]. This fine structure is present in the ionization efficiency curve of CH_3^+ and F^- as observed by Krauss et al.

The next onset for CH_3^+ ion production is determined at 14.50 ± 0.06 eV and corresponds to the mechanism

$$CH_3F + h\nu \rightarrow CH_3^+\left(\tilde{X}\,^1A_1'\right) + F\left(^2P_u\right) + e^- \quad (6)$$

for which the thermodynamic onset is calculated at 14.6 ± 0.3 eV. This reaction has to be correlated with the thermal energy peak observed in the kinetic energy distribution measured at 16.4 eV and at higher energies (see fig. 3). Furthermore the kinetic energy dependence on the appearance energy related to this process shows a slope of 0.53 (straight line (2) in fig. 5) with a correlation coefficient of 0.995. This value being close to the calculated slope of 19/34 = 0.56, it implies that the dissociation occurs with total conversion of the excess energy into translational energy of the fragments.

As underlined earlier [4], this process arises in an energy range where no direct ionization cross section is observed for CH_3F [8]. In spite of its relative intensity, it has not been detected in photoion-photoelectron coincidence experiments [3]. However, the thermal CH_3^+ ions are observed in fixed wavelength photoionization using He(I) and Ne(I) resonance lines [4,5]. Consequently, the occurrence of reaction (6) was ascribed to the

Published in: Chemical Physics (1987), vol. 117, pp. 305-313.
Status: Postprint (Author's version)

population of the same dissociation continuum via autoionizing states.

In the present photoionization work, the photon energy could be scanned continuously from 16.4 to 25 eV, i.e. from the ionization energy of the $CH_3F^+(\tilde{A}^2A_1 + \tilde{B}^2E)$ state up to the $\tilde{C}^2A_1$ state. Besides direct ionization, broad and structureless autoionization continua dominate the ionization events. At all chosen wavelengths, corresponding to maxima and minima in the CH_3F^+ ionization efficiency, the same thermal peak is observed. This would mean that at all these wavelengths the dissociation limit at 14.50 eV is populated via autoionizing states. This CH_3^+ producing process shows a maximum at 15.6 eV. In this energy range (see fig. 1 and 2) the same feature is observed in the photoabsorption curve of CH_3F and in the ionization efficiency curves of CH_2F^+ and CH_2^+.

The third onset in the CH_3^+ ionization efficiency curve is measured at 16.10 ± 0.06 eV. Compared to the corresponding electroionization result [4], this is about 0.3 eV lower. In both experiments the kinetic-energy versus appearance-energy diagram is a vertical Une (the straight Une (3) in fig. 5). As shown earlier [4], the only energetically allowed process for the CH_3^+ ion formation at 16.10 ± 0.06 eV is

$$\mathbf{CH_3F} + h\nu \rightarrow \mathbf{CH_3^+}\left(\tilde{\mathbf{X}}\,^1\mathbf{A_1},\ v\right) + \mathbf{F}\left(^2\mathbf{P_u}\right) + \mathbf{KE} + \mathbf{e}^-, \quad (7)$$

for which the lowest onset (v = 0, KE = 0 eV) is calculated at 14.6 ± 0.3 eV. It occurs at the expense of the $CH_3F^+(\tilde{A}^2A_1 + \tilde{B}^2E)$ state [3-5]. As shown by the dependence of the threshold energy on the kinetic energy, the excess energy of 1.5 eV with respect to the calculated dissociation limit has to be partitioned between vibrational energy v of CH_3^+ and translational energy carried away by CH_3^+ and F.

The kinetic energy distribution of CH_3^+ ions at 16.40 eV (fig. 3a) shows a long high-energy tail in the peak centered at 0.0 eV, which spreads up to 1.0 eV, i.e. 1.0 x 34/19 = 1.79 eV in terms of total energy. The intensity is due to the superposition of CH_3^+ ions distributed (i) from 0 to 0.7 eV and having their onset at 14.50 eV and (ii) from 0 to 1.0 eV with an onset at 16.10 eV. For photon energies of 16.67-16.85 eV (Ne(I) resonance Unes; see fig. 8 in ref. [4]) and 17.3 eV (see fig. 3b) the high-energy distribution clearly peaks at 0.8 eV and extends up to 1.5 eV, i.e. 2.70 eV total energy. The position of the maximum remains constant at 0.8 eV and spreads out to 1.8 eV, i.e. 3.22 eV total energy, for photon energies up to 21.22 eV (see fig. 3c-3e).

The noticeable change of shape of the high-energy distribution between 16.40 and 16.85 eV or 17.3 eV has probably to be ascribed to the contribution of a second electronic state of CH_3F^+ which would have its ionization energy between 16.4 and 16.85 eV. By electroionization, the break-off in the vertical Une (3) at 17.1 eV for kinetic energies of 1.4-1.7 eV was tentatively ascribed to the onset of the contribution of a second electronic state, e.g. the $CH_3F^+(\tilde{B}^2E)$ state. All along this section, it has been pointed out that at this energy of 17.1 eV, thresholds were also measured in both the ionization efficiency curves of CH_2F^+ and CH_2^+.

Finally a weak and broad peak is observed in the ionization efficiency curve of CH_3^+ with a maximum at 19.5 eV and spreading from 19 to 22 eV. The presence of the same feature in the photo-absorption curve of CH_3F, and in the photoionization efficiency curves of CH_3F^+, CH_2F^+ and CH_2^+ strongly suggests that the same Rydberg ($4a_1 \rightarrow 3s$) state autoionizes leading to the four ionized species.

5. Conclusion

The use of synchrotron radiation allowed us to study the photoabsorption curve together with the mass spectrometric photoionization of CH_3F in the photon energy range 10-25 eV. The dissociation channels leading to the CH_2^+, CH_3^+ and CH_2F^+ ions were examined. Whereas the CH_2^+ ionization efficiency curve is discussed without ion energy analysis, owing to its low intensity, the CH_3^+ ion formation is analysed as a function of the translational energy of the ion. Besides energetic CH_3^+ ions, with an onset at 16.1 eV, thermal CH_3^+ ions are evidenced with an onset at 12.45 eV (ion-pair formation) and 14.50 eV (dissociative autoionization). The latter process was missed in earlier photoionization work [2]. The CH_2F^+ ionization efficiency curve has been included and discussed. For the three abovementioned dissociation channels, the major importance of dissociative autoionization has been evidenced.

The present work also shows the feasibility of a dissociative photoionization experiment coupled with ion energy analysis. Translational energy distributions of ions are measured at different wavelengths and

ionization efficiency curves are recorded at different retarding potentials. A kinetic-energy versus appearance-energy diagram has been obtained for the CH_3^+ ion.

Though electroionization is often considered as being less appropriate to study dissociative ionization processes, the comparison made in the present study clearly showed the good agreement between electroionization and photoionization work.

Acknowledgement

Financial support of the Bundesministerium für Forschung und Technologie and of the Belgian Government through an Action de Recherche Concertée (ARC) is gratefully acknowledged. One of us (RL) wishes to thank the Fonds National de la Recherche Scientifique and the Université de Liège for a traveling grant.

References

[1] V.H. Dibeler and R.M. Reese, J. Res. Natl. Bur. Stand. 54 (1955) 127.

[2] M. Krauss, J.A. Walker and V.H. Dibeler, J. Res. Natl. Bur. Stand. A 72 (1968) 281.

[3] J.H.D. Eland, R. Frey, A. Kuestler, H. Schulte and B. Brehm, Intern. J. Mass Spectrom. Ion Phys. 22 (1976) 155.

[4] R. Locht and J. Momigny, Intern. J. Mass Spectrom. Ion Processes 71 (1986) 141.

[5] J. Momigny, R. Locht and G. Caprace, Intern, J. Mass Spectrom. Ion Processes 71 (1986) 159.

[6] R. Locht and J. Momigny, to be published.

[7] W.R. Harshbarger, M.B. Robin and E.N. Lassettre, J. Electron Spectry. 1 (1973) 319.

[8] L. Karlsson, R. Jadrny, L. Mattsson, F.T. Chau and K. Siegbahn, Phys. Scripta 16 (1977) 225.

[9] G. Bieri, L. Åsbrink and W. von Niessen, J. Electron Spectry. 23 (1981) 281.

[10] G. Herzberg, Molecular spectra and molecular structure. Vol. 3 (Van Nostrand, Princeton, 1967).

[11] C.F. Bender and H.F. Schaefer III, J. Mol. Spectry. 37 (1975) 423.

[12] C. Galloy and J.C. Lorquet, Chem. Phys. 30 (1978) 169.

[13] D.H. Liskow, C.F. Bender and H.F. Schaefer III, J. Chem. Phys. 61 (1974) 2507.

[14] S. Tsuda, C.E. Melton and W.H. Hamill, J. Chem. Phys. 41 (1964) 689.